

**Seismic sources and structure in Iran and the Caucasus from Joint Seismic
Program Array Data**

G.A. Abers¹, W.-Y. Kim², and A. Lerner-Lam²

¹Department of Geology, University of Kansas, Lawrence KS 66045

²Lamont-Doherty Earth Observatory of Columbia University, Palisades NY 10964

Contract No. F49620-95-1-0002

Sponsored by AFOSR

ABSTRACT

Amplitudes of seismic waves recorded at the Caucasus network, along the north flanks of the Greater Caucasus, are measured and analyzed for attenuation characteristics. From one year of observation, 96 events between 1° and 10° from the network provide stable measures of RMS P_n , S_n , L_g , and late coda amplitudes. Measurements were taken from seismograms filtered at several narrow frequency bands centered from 0.5 to 8.0 Hz, where signal levels are highest. Our results confirm previously-inferred spatial variations in S_n and L_g attenuation, that the Greater Caucasus marks an abrupt boundary between the high- Q Russian Platform and a region of exceedingly poor S_n and L_g propagation within the collision belt. Paths that cross large Quaternary volcanic provinces, along the Greater Caucasus, seem most affected. Amplitude ratios show the largest regional differences in the 1-2 Hz range and decrease at higher frequencies, and indicate complicated changes in the mechanism of attenuation between shield and tectonic paths.

For a given path the RMS amplitudes of the L_g group and late coda phases predict magnitudes as well as can be expected from mb uncertainties. However biases of 1.0-1.5 magnitude units are seen for RMS amplitudes along different paths, at frequencies higher than 1 Hz. Variation is much reduced by taking 3-component and network averages of amplitude measurements.

Keywords: attenuation, regional seismic waves, magnitudes, Caucasus region

19960624 157

OBJECTIVE

We evaluate and characterize seismic data from digital network and array sites in and around the Former Soviet Union, in order to provide new constraints on seismic wave propagation characteristics in the Caucasus Ranges, Middle East and Iranian Plateau. Strong changes in the attenuation and velocity behavior of seismic waves are associated with the mountain belts here, and make it difficult to infer wave behavior from experiences gained within stable cratons. Seismograms from the JSP-Caucasus Seismic Network collected since 1991 include a large number of local and regional events in the region. These waveforms are used for assessing the amplitude and phase of major wave groups along regional paths, and constraining earth structure beneath the network. Results provide information on the behavior of common event discriminants and detection thresholds for regional paths.

RESEARCH ACCOMPLISHED

Severe changes in wave behavior are observed between paths that cross the Caucasus and other Alpine-Himalayan mountain belts, and those that do not (Figure 1). These changes represent substantial attenuation of phases often used to discriminate explosions from earthquakes and to estimate event size and type, such as *Lg* and other high-frequency surface-related phases. Work to date has concentrated on quantifying the behavior of seismic waves as they cross the Caucasus, mostly by examining phase amplitudes for events within 10° of the Caucasus Seismic Network (CNet). Other facilities, such as the Geyokcha, Turkmenistan array, the array in Garni, Armenia, and the Iran Long Period Array also provide digital seismograms that can give complementary information.

Caucasus Network

The Caucasus network was established in 1991 through the Joint Seismic Program, as a cooperative project between Lamont-Doherty and the OME-Obninsk group (Abers, 1994). The network, based in Kislovodsk (KIV), consists of 5-6 digitally telemetered 3-component sensors with 0.2 Hz natural periods, digitized at 60 sps. These stations are on the north side of the Greater Caucasus range, and straddle the transition from the Russian Shield to the Caucasus collisional zone. The northern stations lie on flat-lying, poorly consolidated Neogene sediments, while southern stations lie on tilted, well-lithified Mesozoic sediments. The response of the Kinemetrics SV/SH sensors are well-suited for analysis of local and regional seismic waves, although prior to mid-1993 triggering windows usually did not include *S* or *Lg* for events farther than 10 - 15° from the network. We are in the process of extracting seismograms from a continuously-recording backup system in order to produce a waveform data set suitable for these longer distances. Data for 1992 were picked and associated by the Joint Seismic Program Center (Harvey et al., 1994) and subsequent seismograms are distributed through IRIS. A total of 645 events were associated for 1992 (292 in the PDE), and 327 were associated with the PDE catalog in 1993.

RMS Amplitudes of Regional Phases

We have measured RMS amplitudes of *P*-group, *S*-group, *Lg* and similar, and late coda from recordings of events 1 - 10° from CNet. Because the CNet time series contain occasional spikes and, at some stations, frequent telemetry gaps, spectral methods are often problematic. More robust amplitude estimates are made from RMS amplitudes of multiple-narrow-band signals. For each seismogram, a series of narrow-band filters are constructed and applied centered at 0.5, 1.0, 2.0, 4.0, and 8.0 Hz. For each channel and frequency, RMS amplitudes are made in several time windows: pre-event noise, *Pn*, *Sn*, *Lg*, and coda. *Pn* and *Sn* windows extend from 4 s before the predicted phase onsets to 0.25 times the *S-P* time past the onset, up to 25 s in total length. The so-called *Lg* window covers the period in group velocity between 3.6 and 2.6 km/s; the range extends to slower than normal group velocities to include the dominant slow short-period surface phases observed for shield paths (Figure 1). The coda window is centered at twice the *S* travel time after

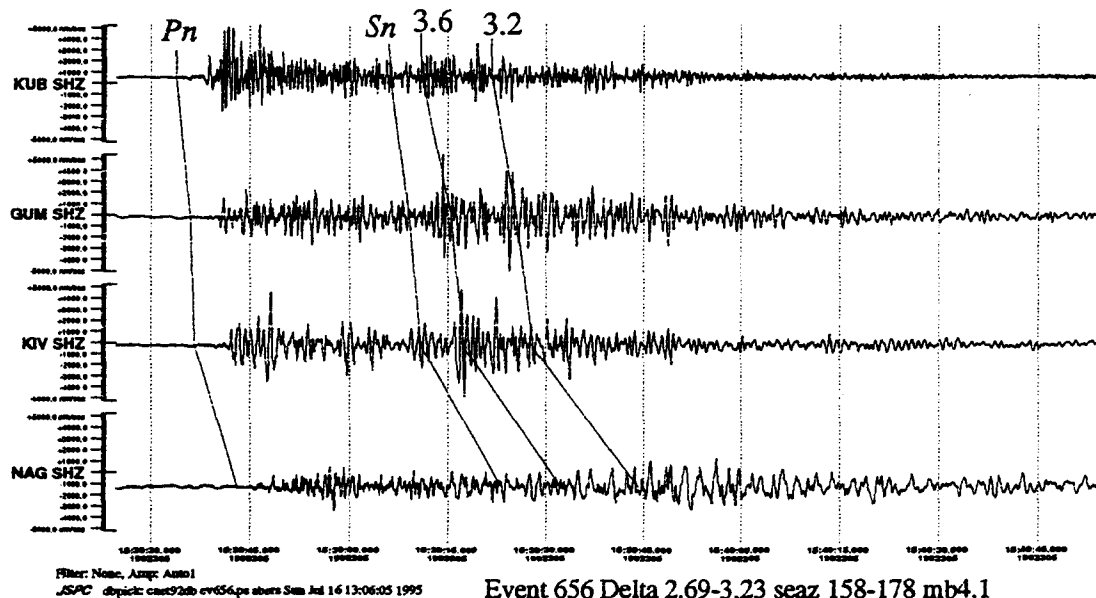
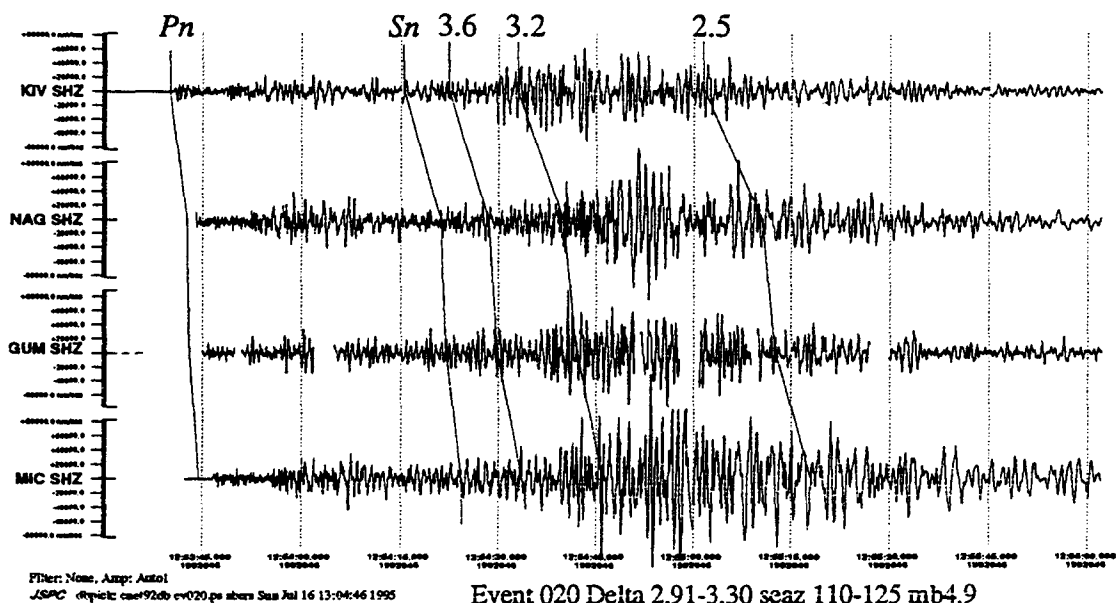
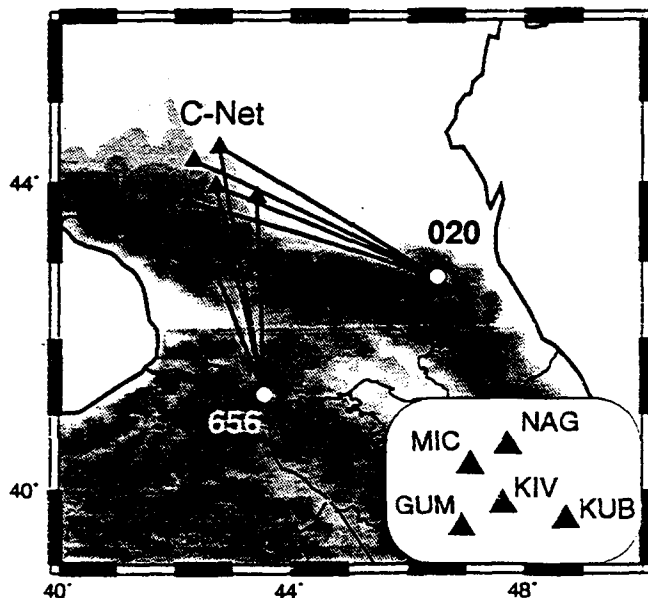


Figure 1. Records from two events from $\sim 3^\circ$ distance recorded at the Caucasus network. Waves for event 020 in Dagestan, top, travel largely on the Russian platform margin while waves for event 656, bottom, cross the Greater Caucasus and Kura basin. Seismograms are labeled by arrivals of P_n , S_n , and group velocities in km/s. Note absence of late-phase energy on lower traces, particularly in and after L_g window (after 3.6 km/s). Event 020 shows small P_n relative to S_n and late phases, and slow high-frequency surface waves (< 3 km/s).



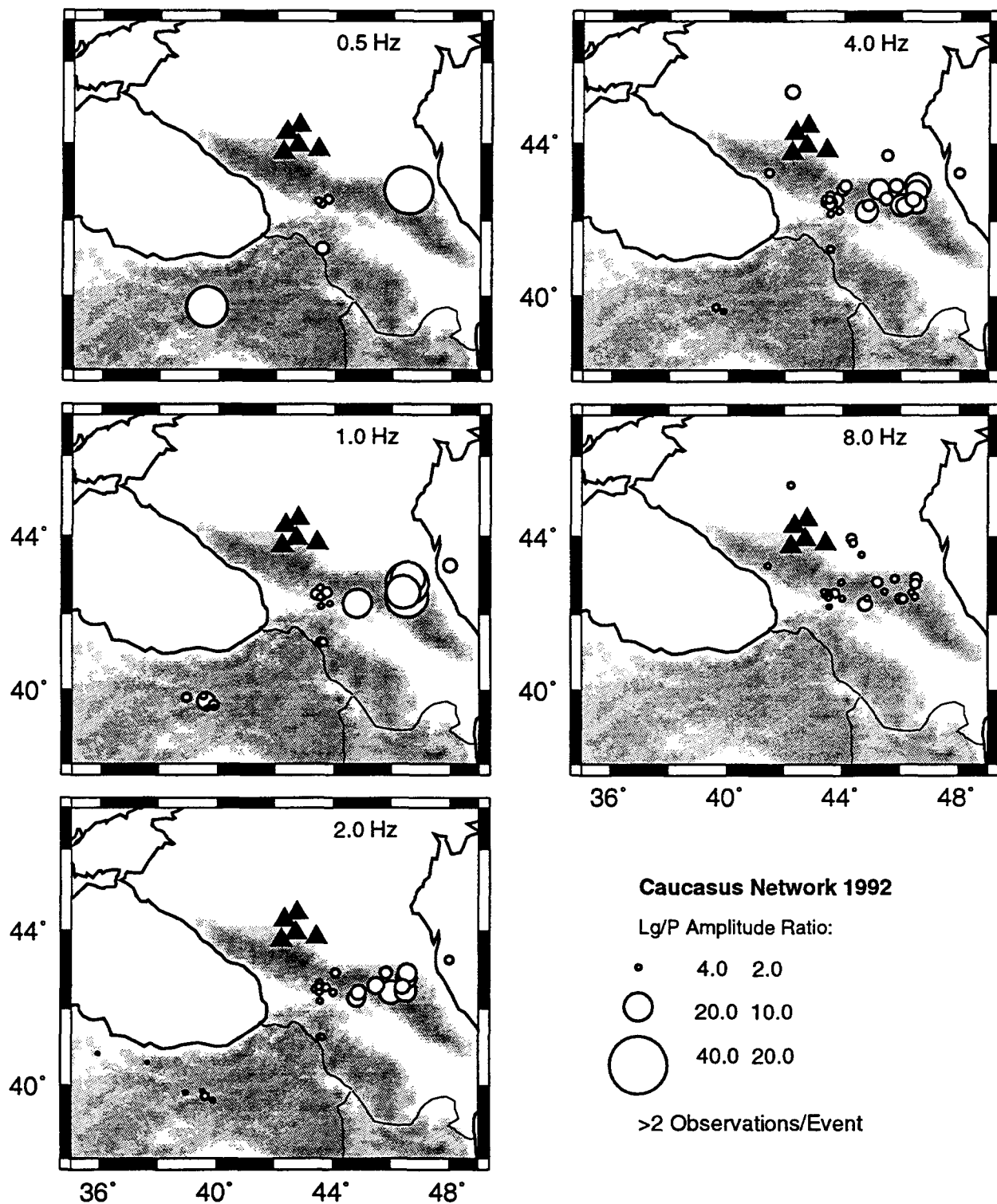


Figure 2. Ratios of RMS-Lg amplitude to P amplitude for events 1-10° from CNet, 1992. Each panel represents a different frequency seismogram, labelled top. Three-component RMS amplitudes are averaged over the network geometrically, and only shown when 3 or more stations are used. Symbols are centered on events. Size of symbols scales to amplitude ratios, as by key at lower right (left-hand and right-hand numbers are for left and right column of figure, respectively).

the origin time, and is 40 s in duration. Only segments that were more than 4 s long are used, and only those where dropouts constituted less than 10% of the time window. These requirements allow some data where short trigger-windows or occasional dropouts might be present, and because the RMS measurements are integrated quantities the measurements are still valid. All seismograms are visually culled for other, unusual problems.

An RMS combination is made of measurements from each 3-component seismogram set, for as many components as were usable. Signal-to-noise estimates are made on these combined sets, and records with low (<2) signal level signals are eliminated. Noise estimates are made from each filtered seismogram, where possible, or instead taken as the maximum observed RMS noise level for a particular channel and frequency. Amplitudes are corrected in an RMS sense for incoherent noise contamination. Finally, amplitudes are averaged geometrically across the network for each event (and across all events for each station) to give a network-average set of amplitude ratio estimates. Only averages of three more stations are kept. These averages were considerably less variable than single station estimates.

Results

In map view (Figure 2) large variations in amplitude ratios are seen between paths that cross the crest of the Greater Caucasus and those that do not, and indicate extensive *Lg* blockage and *Sn* attenuation throughout the actively deforming parts of the Caucasus belt. Such behavior was seen by Kadinsky-Cade et al. [1981], although they did not have access to stations north of the Caucasus and were limited to analog records. Using some of the same Caucasus Network data Rodgers et al. [1994] saw a region of poor *S* and *Lg* propagation beneath the Caucasus. Our results document the frequency dependence of this phenomenon, and (similar to Rodgers et al.) show that the boundary of the attenuative region is sharp and lies beneath the core of the Greater Caucasus. Results are most consistent for the *Lg* window although the *Sn* window behaves similarly. Differences are most pronounced at lower frequencies (Figure 3).

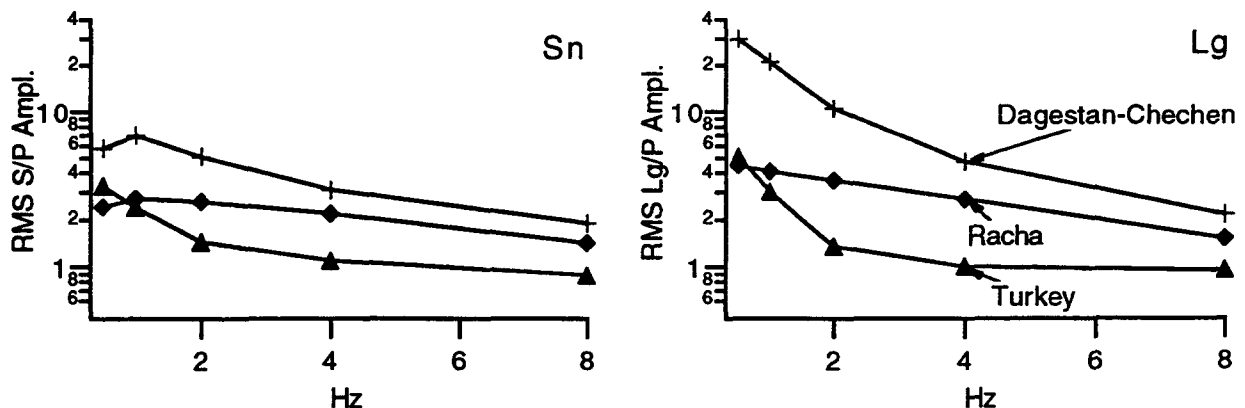


Figure 3. Variation in RMS amplitude ratios as a function of frequency for three regions. Regions on Figure 4.

Paths from events in the Dagestan-Chechnya region (DA, Figure 3,4) are roughly parallel to the strike of the ranges and follow the margin of the mountains and traverse thick foredeep sediments north of the Greater Caucasus. These paths are also characterized by slow (~ 2.9 - 3.0 km/s) high-frequency Rayleigh waves (Figure 1). Large amplitudes are seen most frequencies, particularly from 0.5 to 2 Hz, and may reflect the a layered, relatively undisrupted nature of the paths.

Paths that cross the Greater Caucasus show very low-amplitude *S* and *Lg*-related phases relative to the *P* arrivals, even for relatively short paths. Many events are roughly 200 km distant, near the 1991 Racha earthquake zone (Triep et al., 1995), yet show amplitude ratios 3-10 times lower than for Dagestan paths. Waves from these events traverse the active deformation front of the Greater Caucasus, and the region of Plio-Quaternary volcanism near Mt. Elbruz at the SE edge of the network. Paths from events farther south that traverse the Lesser Caucasus show very small-amplitude late phases.

Absolute RMS amplitudes for a given region correlate well with event size measures such as m_b (Figure 4) although the scaling parameters vary systematically between regions. The m_b values come from the PDE for region TU, and from the CNet Information Product for closer events (so that some coupling with RMS P_n is expected). In general correlation coefficients are 0.8-0.9 for each population between 1 and 4 Hz. Events from Turkey show RMS amplitudes of late phases a factor of 10-100 low at 2 Hz compared with shield paths, with the discrepancy increasing with frequency. Some of the best correlations (>0.9) come from late coda amplitudes, which have long been used for magnitude determination in the Caucasus (Rautian et al., 1979). The variation from region to region corresponds to biases of 1.0-1.5 magnitude units in the ability of 2-Hz L_g , S_n , or coda to predict m_b .

Variation is also seen between stations consistently for all events (not shown). The stations farthest onto the platform show consistently large L_g/P_n and S_n/P_n amplitude ratios by a factor of 1.7-2.5 relative to stations at high elevation, as well as the largest absolute amplitudes. The large amplitudes can be attributed to low velocities of Neogene near-surface sediments that lie beneath the platform stations.

CONCLUSIONS AND RECOMMENDATIONS

Reduction in high-frequency seismic wave amplitudes across Eurasian collision zones appears to be associated with a highly localized boundary that follows the northern margin of the Greater Caucasus. Events in the Racha region, on the southern flanks of the Greater Caucasus, show reduction in L_g/P and S/P amplitude ratios comparable to more distant events that cross the entire region. Although amplitude ratios seem stable for paths from individual regions, as evidenced by the good correlations with m_b , the attenuation effects are highly variable. A spatially-varying attenuation model for the region is necessary in order to utilize L_g/P_n and S_n/P_n discriminants as these amplitude ratios vary by over a factor of 5-20 between different paths. The amplitude reduction, seen throughout the 0.5-4 Hz band, suggests that signals will be small for small regional events in the Caucasus-Iranian Plateau region, relative to comparable paths along shield sites. Robust measurements seem to require both 3-component analysis and averaging over several nearby stations, both done here. Future work should include developing a data set of long seismograms appropriate to studying L_g and S -group energy at 10-20° distances, quantifying frequency-dependent Q in a way that can be used for path calibration, and adding complementary observations from other networks and arrays.

REFERENCES

- Abers, G.A., The Caucasus Seismic Network, *IRIS Newsletter*, 13, 1994.
- Harvey, D, and others, Caucasus Network Information Product Triggered events from January 1, 1992 to November 9, 1992, Version 1.0, IRIS-JSPC, 1994.
- Kadinsky-Cade, K., M. Barazangi, J. Oliver, and B. Isacks, Lateral variations of high-frequency seismic wave propagation at regional distances across the Turkish and Iranian plateaux, *J. Geophys. Res.*, 86, 9377-9396, 1981.
- Rautian, TG, VI Khalturin, and IS Shengeliya, Seismic coda envelopes and assessment of earthquake magnitudes in the Caucasus, *Phys. Solid Earth*, 15, 393-398, 1979.
- Rodgers AJ, TM Hearn, and JF Ni, P_n , S_n and L_g propagation in the Middle East, *EOS Trans AGU*, 75(44), 463, Fall, 1994.
- Triep, E., G.A. Abers, A. Lerner-Lam, V. Mishatkin, N. Zhacherenko, and O. Staravoi, Active thrust front at the south slope of the greater Caucasus: The 29 April, 1991 earthquake and its aftershock sequence, *J. Geophys. Res.*, 100, 4011-4034, 1995.

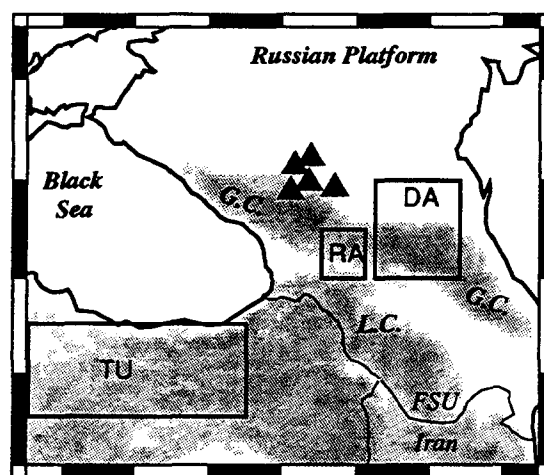
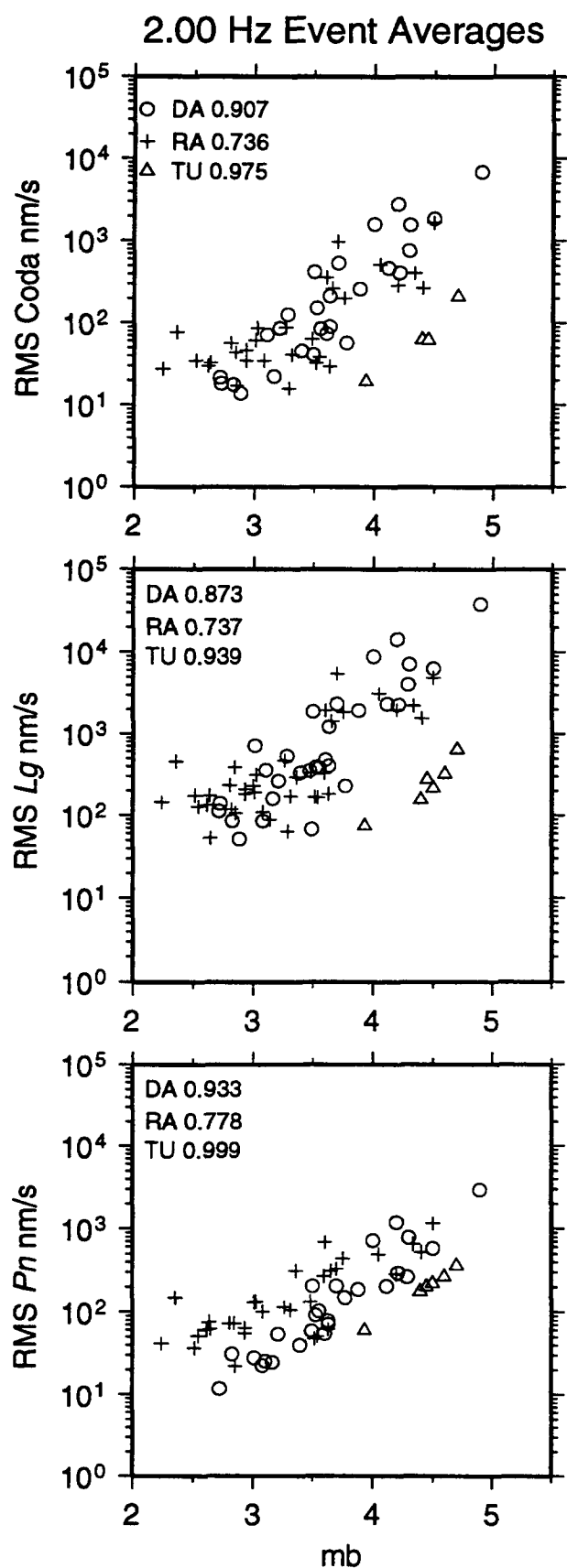


Figure 4. Right shows three-component RMS amplitudes of 2-Hz wavetrain vs. mb estimates. Coda is 15-30 s window centered at twice the S wave travel time, Lg window spans 3.6 to 2.6 km/s group velocity, and Pn window extends to 25% of $S-P$ time. Signal-to-noise ratios exceed 2.0 for all measurements, and measurements are averaged over 3 or more network stations. Different symbols correspond to events from different regions as labelled: DA - Dagestan-Chechnya; RA-Racha aftershock zone; TU-Turkey. The mb value is taken from PDE for TU and from JSPC measurements on Caucasus events (Harvey et al. 1994) for closer regions. Correlation coefficients between $\log(\text{amplitude})$ and mb are also shown in upper left of each plot. Correlations for individual paths are good although significant variations exist between regions. Amplitudes are corrected for cylindrical geometric spreading to nm/s at 100 km. Map, top right, shows region areas as well as: G.C. - Greater Caucasus, L.C. - Lesser Caucasus.